Iranian Journal of Physics Research, Vol. 24, No. 3, 2024
DOI: 10.47176/ijpr.24.3.31863

Space weather disturbances and their geoeffectiveness during solar cycle 23 and 24

Sh Singh
Chandigarh Engineering College-CGC, Landran, Mohali-140307 India

E-mail: shamrathore@yahoo.com

(Received 06 March 2024 ; in final form 23 August 2024)

Abstract
We present the findings of a study of the sequence of solar activity that eventually resulted in 80 large geomagnetic storms (distinguished by minimum Dst -100nT to -200nT), 11 super geomagnetic storms (Dst -200nT to -300nT), and 6 super great geomagnetic storms (Dst -300nT) that occurred between 1996 and 2012. Large storms were discovered to be mostly caused by solar flares (M- and X-class), while corotating interaction region (CIR) was also a significant contributor to several of these storms. During the peak and declining phases of solar cycle 23, all extremely powerful storms were observed (2000-2004). It has been noted that coronal mass ejections (CMEs) and flares were always related with super and super tremendous storms (100%). M-class and X-class flares frequently accompany superstorms associated to CMEs. It is observed that 66.6% (4/6) super great geomagnetic storms (Dst ≤ -300nT) were associated with CMEs and solar flares. The number of storms related to X-class flares or CMEs were 50% (3/6). X-class flare/CMEs are found to be responsible for super geomagnetic storms.

Keywords: solar flares, interplanetary magnetic field, coronal mass ejections, geomagnetic storms

1. Introduction

The disruption in the Earth's magnetic field is caused by solar output, namely the release of solar plasma and magnetic field into the interplanetary medium. When ionization is produced in the planet's sun-drenched region, these plasmas and fields interact with the Earth's atmosphere, and the geomagnetic field experiences unusual storm-time alterations. The large disturbances in Earth's magnetic field are known as geomagnetic storms. They frequently last for many days or more. The magnetic field measured at Earth's surface is disturbed by powerful electric currents flowing through the magnetosphere and ionosphere, the aurora brightens and extends to low magnetic latitudes, and the magnetosphere experiences tremendous fluxes of energetic charged particles. The sun is the main factor influencing solar storms, which affect Earth's atmosphere. Storms on the Sun, such as solar flares and coronal mass ejections (CMEs), can project strong magnetic fields and radiation showers into the space between planetary systems and change the ever-changing ambient conditions in our Earth atmosphere. There is a close connection between the coronal mass ejections and the other types of solar activity that we see on the sun. Similar to other indices of solar activity, the rate of mass ejections varies during the course of the 11-year solar cycle [1-3]. Sunspots and other solar events are strongly correlated with changes in the Earth's magnetic field, and they have a variety of consequences on the upper atmosphere [4-7]. Temperature, air pressure, wind direction and speed, humidity, precipitation, and also other factors are among its constituents. The constantly shifting ambient conditions in the space of our solar process are defined as space weather. Some of its components are electromagnetic radiation, the solar wind of charged particles that the Sun emits, and the intensity of the interplanetary magnetic field (IMF), which spirals outward from our planet star. The interplanetary causes of large storms (Dst ≤-100 nT) during solar cycle 23 have been investigated by many authors [8-10]. Interplanetary space probes have recorded increased wind speeds and densities as well as a rapidly changing magnetic field when they have encountered such disturbance. Geomagnetic storms are created when these planetary disturbances reach the Earth. The solar cycle affects how frequently they occur. At solar maximum, there are averages of two or three CMEs per day, compared to around one per week at solar minimum. Because they can send powerful southerly fields to Earth near the dayside boundary of the magnetosphere, coronal mass ejections have the potential allowing solar wind energy, momentum, and mass access to the magnetosphere makes them geoeffective in the sense that they will have the ability to cause geomagnetic storms [11-13]. Geoeffectiveness is

determined by CME speed [14-16]. Speed changes significantly more than the other regulating element, the strength of the southerly magnetic field, therefore its total impact on storm strength as an electric field factor is not significant. CME that moves more quickly than the ambient solar wind is more effective from a geophysical standpoint because it compresses any southern fields on its leading edge [17-18]. The most geoeffective solar wind perturbations are caused by CMEs Research on CMEs provides information on their geoeffectiveness as well as other CME-related topics [19-27]. CME characteristics [28, 29] and flares associated with CMEs [30, 31]. A moderate positive correlation between SEPs and flares as well as CMEs is found [32]. Mohammadi [33] shows that both western solar longitude large flares (X-class, M-class) and flares associated with coronal mass ejections (with speed greater than 500 km s^{-1}). The magnetic field of the Sun is also carried by the solar wind. Either the North or the South will be the direction of this field. Geomagnetic storms can be anticipated if the solar wind experiences intense bursts that contract and stretch the magnetosphere or if the solar wind adopts a southerly polarity. The dayside magnetopause is magnetically reconnected as a result of the southern field; releasing magnetic and particle energy into the magnetosphere of the Earth quickly. The ionosphere's F-2 layer will become unstable during a geomagnetic storm. It is possible to see auroras in the sky near the Earth's northern and southern poles. For extended periods of time, a number of authors have researched the geoeffectiveness of magnetic clouds [34-37]. The local topography affects the local weather when a cold front on Earth comes into contact with a mountain range. Similar to this, when a CME-generated powerful pulse in the solar wind collides with Earth's magnetic field, the solar wind and Earth's magnetosphere interact in complicated ways to affect the storm's overall effects on the Earth and in the region around it. Some of our space weather appears as brief storms, which can persist for a few seconds, minutes, hours, or even days [38-39]. Longer-term fluctuations in space weather result from cycles in the sun's activity level that last years to decades. The Sun has altered significantly during the course of our solar system's multi-billion-year history, causing long-term "climate change" consequences in our space weather. However, a number of geomagnetic indicators have been created for global quantitative representation. The disturbance storm time provides a predictable way to assess the ring current energy and intensity over low and intermediate latitudes. (Dst index). The H fluctuations measured at middle and low latitude observatories are averaged longitudinally to provide the Dst values. It is the most accurate measure of ring current strengths and a highly sensitive indicator of the severity of solar disturbances. The energy that is dissipated in the ionosphere and the energy of electrons that are precipitated on the auroral and polar areas are measured by the auroral electrojet magnetic intensity index (AE), which was first introduced by Singh and Tsurutani in [23,34]. The global geomagnetic activity was assessed using the planetary global indices Kp and Ap. The planetary index Ap, which is frequently used in several disciplines of science to define the status of the geomagnetic field, measures the level of daily global geomagnetic fluctuation. The geomagnetic storm, commonly referred to as the storm time variations, discusses the many features of geomagnetic storms and how they relate to solar source activity and planetary magnetic fields [40]. Geomagnetic storms, caused by the boosted solar wind and its interaction with the Earth's magnetosphere-ionosphere-thermosphere system, can have significant impacts on power grid infrastructure in mid-latitude regions [41].

These changes have a direct impact on humans and have a negative impact on satellites, communications, and power losses [42-43]. Effect of geomagnetic storms on a power network at mid latitudes [44].

The statistical analysis in this paper aims to define how solar plasma interacts with the geomagnetosphere and influences the upper atmosphere. Large geomagnetic storms that are extremely dangerous to humans and that have an impact on our electrical grid, pipelines, satellites, and space weather have been examined in the current work [45]. We selected a lengthy time frame (1996–2012) for this analysis, which includes solar cycles 23 and 24. The study of solar cycle 23 has unique importance because of the occurrence of large geomagnetic storm during its declining phase. This work provides a better understanding of the space weather phenomena by describing various geomagnetic disturbance types and their potential solar and planetary causes.

2. Selection criteria and data sources

A set of art of geomagnetic field variation and morphology of geomagnetic storms are presented in this paper. Different types of geomagnetic indices are used to calculate the change in geomagnetic field variations. The data of geomagnetic indices are available on different geomagnetic observatories. Some geophysical networks provide complied data. The geomagnetic disturbances can be observed at various locations of the Earth’s surface such as polar, mid-latitude and equatorial regions. These geomagnetic disturbances are generally observed and represented by different geomagnetic indices.

In the current study, I have compiled a list of every standard type of geomagnetic storm that was observed between 1996 and 2012, which includes the solar cycle 23 and solar cycle 24 maxima, and that was associated with Dst decreases of more than -100nT to -200nT (large storm), -200nT to 300nT (super storm), and less than -300 nT (super-great storms). The value will range from between -100nT to -500nT at its lowest point during a storm. The major phase lasts between two and eight hours on average. Dst transitions from its minimal value to its quiet time value throughout the recovery phase. The duration of the healing phase can range from 11 hours to 7 days. When the storm's Dst value recurs for multiple consecutive days or hours, we have calculated geomagnetic storms, and the most recent day or hour is used to determine the storm day or hour. The limitation to this category of storms produced a constrained group of events appropriate for a thorough investigation. Based on two-time markers, the start of the main phase of geomagnetic storms is determined. One is related to the storm's SSC hour, while the other is the start of the major

phase. The hour after Dst values fall below the mean Dst of the preceding date is known as the main phase beginning. Even though the daily mean is typically close to zero, it could occasionally be a few nT either way. The accuracy of main phase onset time has been believed to be about ±2 hours [24]. The geomagnetic storm is not deemed to be over until the hourly Dst values remain at a relatively steady level for several hours. However, if the storms are clearly visible in the hourly plot and meet the criteria for selection, they have been treated as separate storms from those that occurred during the prior event's recovery phase. The total lifetime of a storm variation in the interval between the associated storm sudden commencement/main phase onset and hour of storm ending.

We have investigated how storms relate to various solar and planetary disturbances and how they relate to one another. The U.S. Department of Commerce's Solar Geophysical Data (Prompt/Comprehensive report), NOAA, and Omni web data were used to obtain the geomagnetic index hourly data. The various geomagnetic, interplanetary and solar data measured through a number of satellites and observatories have been obtained from either on request to concerning authority or by internet. During our study period, we find that Moderate, Large, Super, Super- great geomagnetic storms and their association with CMEs or flare are falling under our section, and are listed in Tables as 1, 2 and 3. Different columns of the table present specific feature of large geomagnetic storm given as:

Column (1) Serial number of large geomagnetic storm.
Column (2) Observed date of large geomagnetic storm.
Column (3) Time of Event
Column (4) Maximum decrease in Dst values (nT).
Column (5) Initial phase duration (hours).
Column (6) Main phase durations (hours).
Column (7) Recovery phase durations (hours).
Column (8) Longevity of storm (hours).
Column (9) Association with CMEs speeds (km/s)
Column (10) Association with flare
Column (11) Association with CIRColumn
Column (12) Types of CMEs

Table 1. List of large geomagnetic storms.

Storm No.	Date of maximum decreases in Dst value	Time of Event	Magnitude of storm ≤-100 to -200 (nT)	Initial Phase duration (hrs)	MainPhase duration (hrs)	Recovery Phase duration (hrs)	Longevity of storm (hrs)	Asso.with CMEs speeds (km/s)	Asso. with Flares	Asso. with CIR	Types of CMEs
1	2	3	4	5	6	7	8	9	10	11	12
Solar Cycle 23								1996			
01	Jan.13	04UT	-105	06	02	100	108	No CMEs	No Flare	CIR	--Nil--
1997											
02	April 21	23UT	-107	10	02	33	45	No CMEs	No Flare	CIR	--Nil--
03	May 14	12UT	-115	05	05	72	82	No CMEs	No Flare	CIR	--Nil--
04	Oct. 11	03UT	-130	07	06	94	107	1271	No Flare	--Nil--	PH
05	Nov. 07	04UT	-110	04	02	54	60	1556	X94	--Nil--	H
06	Nov. 22	12UT	-108	07	05	89	101	951	No Flare	--Nil--	--Nil--
1998											
07	Feb. 02	00UT	-100	10	01	80	91	No CMEs	No Flare	CIR	--Nil--
08	March 10	20UT	-116	07	07	80	94	760	No Flare	--Nil--	-Nil---
09	June 26	04UT	-101	04	01	34	39	No CMEs	No Flare	CIR	--Nil--
10	Aug. 06	11UT	-138	08	03	72	83	No CMEs	No Flare	CIR	--Nil--
11	Aug. 27	09UT	-155	06	07	132	145	No CMEs	X10	--Nil--	--Nil--
12	Oct. 19	15UT	-112	11	02	88	91	No CMEs	M24	--Nil--	--Nil--
13	Nov. 08	06UT	-149	07	02	14	22	1118	M24	--Nil--	H
14	Nov. 09	18UT	-142	14	07	69	90	No CMEs	M27	--Nil--	--Nil--
15	Nov. 13	21UT	-131	12	09	108	129	847	M11	--Nil--	-Nil---
1999											
16	Jan. 13	23UT	-112	08	05	99	112	No CMEs	No Flare	CIR	--Nil--
17	Feb. 17	09UT	-123	05	09	72	186	758	M15	--Nil--	--Nil--
18	Sept. 21	23UT	-173	02	03	68	73	1144	No Flare	--Nil--	--Nil--
19	Nov. 13	22UT	-106	08	02	51	61	789	M11	--Nil--	--Nil--
2000											
20	Feb. 12	11UT	-133	06	02	64	72	944	No Flare	--Nil-	H
21	May 24	08UT	-147	02	06	71	79	794	No Flare	--Nil-	--Nil--
22	Aug. 11	06UT	-106	09	01	18	28	1133	M19	--Nil-	--Nil--

23	Oct. 05	13UT	-182	28	10	91	129	No CMEs	No Flare	CIR	-Nil---
24	Oct. 14	14UT	-107	23	03	63	89	799	M15	--Nil-	--Nil--
25	Oct. 29	03UT	-127	04	03	64	71	964	M11	--Nil-	--Nil--
26	Nov. 07	21UT	-159	07	07	59	73	No CMEs	No Flare	CIR	--Nil--
27	Nov. 29	13UT	-119	20	04	71	95	No CMEs	X40	--Nil-	-Nil---
2001											
28	March 18	13UT	-149	23	07	134	164	No CMEs	No Flare	CIR	--Nil--
29	April 18	06UT	-114	04	04	59	67	720	X10	-Nil--	H
30	April 22	15UT	-102	14	01	61	76	No CMEs	M20	--Nil-	--Nil--
31	Aug. 17	21UT	-105	04	01	36	75	1575	No Flare	-Nil--	H
32	Sept. 25	01UT	-102	03	01	66	70	2402	X26	-Nil--	H
33	Oct. 01	08UT	-148	09	03	48	60	No CMEs	M10	-Nil--	--Nil--
34	Oct. 03	14UT	-166	04	07	46	57	1405	M14	-Nil--	H
35	Oct. 22	21UT	-187	03	29	56	88	901	X16	-Nil--	H
36	Oct. 28	11UT	-157	07	04	73	84	1092	X13	-Nil--	H
37	Nov. 01	10UT	-106	20	02	62	84	716	M15	-Nil--	PH
2002											
38	March 23	09UT	-100	10	01	41	52	1075	M16	-Nil--	--Nil--
39	April 18	07UT	-127	05	07	21	33	1240	M25	--Nil-	H
40	April 20	08UT	-149	20	05	67	92	804	No Flare	--Nil-	--Nil--
41	May 11	19UT	-110	05	03	41	49	1154	No Flare	--Nil-	--Nil--
42	May 23	17UT	-109	05	02	79	86	1557	X21	-Nil--	H
43	Aug. 02	05UT	-102	05	01	43	49	No CMEs	M12	--Nil-	--Nil--
44	Sept. 04	05UT	-109	05	03	49	57	No CMEs	M10	--Nil-	--Nil--
45	Sept. 08	00UT	-181	10	08	149	167	909	No Flare	-Nil--	H
46	Oct. 01	16UT	-176	08	09	37	54	No CMEs	M21	--Nil-	--Nil--
47	Oct. 04	08UT	-146	15	04	57	76	834	M21	--Nil-	--Nil--
48	Sept. 09	07UT	-115	05	02	43	50	846	M10	--Nil-	--Nil--
49	Oct. 14	13UT	-100	22	01	29	52	1009	M22	--Nil-	--Nil--
2003											
50	May 30	23UT	-144	06	05	69	70	1366	X17	--Nil-	H
51	June 18	09UT	-141	06	03	61	70	2053	X13	--Nil-	H
52	July 12	05UT	-105	07	01	33	41	877	M20	--Nil-	--Nil--
53	Aug. 18	15UT	-148	09	11	179	199	814	No Flare	--Nil-	--Nil--
2004											
54	Jan. 22	13UT	-149	07	03	93	103	965	M10	--Nil-	H
55	Feb. 11	17UT	-109	06	02	62	70	No CMEs	M12	--Nil-	--Nil--
56	April 04	00UT	-112	09	02	29	41	No CMEs	No Flare	CIR	--Nil--
57	July 21	02UT	-101	05	01	25	31	790	M11	--Nil-	--Nil--
58	July 23	11UT	-148	09	11	28	48	899	M12	--Nil-	--Nil--
59	July 25	13UT	-197	12	04	85	101	874	M10	--Nil-	--Nil--
60	Aug. 30	22UT	-126	10	04	77	91	1195	No Flare	--Nil-	--Nil--
61	Nov. 12	10UT	-109	02	02	57	61	3387	X	--Nil-	H
2005											
62	Jan. 18	08UT	-121	09	01	62	72	2681	X26	--Nil-	H
63	Jan. 22	06UT	-105	09	03	64	76	1011	X13	--Nil-	--Nil--
64	May 08	18UT	-127	04	06	61	71	1144	M13	--Nil-	--Nil--
65	May 20	08UT	-103	04	01	63	68	No CMEs	M18	--Nil-	--Nil--
66	May 30	13UT	-138	04	04	64	72	786	M11	--Nil-	--Nil--
67	June 13	00UT	-106	03	02	53	58	No CMEs	No Flare	CIR	--Nil--
68	Aug. 31	19UT	-131	04	04	31	39	1600	M16	-Nil--	H
69	Sept. 12	10UT	-147	05	04	86	95	1922	X11	-Nil--	H
2006											
70	April 14	09UT	-111	08	01	43	52	No CMEs	No Flare	CIR	-Nil--
71	Dec. 15	07UT	-146	04	07	76	87	1174	X34	-Nil--	H
2007											
….	…….	……	……	.... Nil….	…….	…….	…….	…..			
Solar Cycle 24								2008			
….	…….	……	……	.... Nil….	…….	……	…….	…..			
2009											
….	…….	……	……	.... Nil….	…….	…….	…….	…..			
2010											
….	…….	……	……	.... Nil….	…….	…….	…….	…..			
2011											

72	Aug. 06	03UT	-113	05	02	51	58	1315	M60	--Nil-	H
73	Sept. 27	23UT	-103	05	03	63	71	1905	X	-Nil--	H
74	Oct. 25	01UT	-137	02	06	81	89	1005	M	--Nil-	H
2012											
75	March 09	08UT	-143	06	07	51	64	2684	X	--Nil-	H
76	April 24	04UT	-104	10	02	48	60	616	No Flare	--Nil-	--Nil--
77	July 15	18UT	-133	07	10	89	106	885	X	--Nil-	H
78	Oct. 01	03UT	-133	12	04	59	75	N.A.	M	-Nil--	--Nil--
79	Oct. 08	12UT	-106	10	03	71	84	N.A.	No Flare	CIR	--Nil--
80	Nov. 14	07UT	-109	12	05	64	81	N.A.	M	--Nil-	-Nil--

Table 2. List of super geomagnetic storms.

Storm No.	Date of maximum decreases in Dst value	Main Phase onset date (hrs)	Magnitude of storm ≤-200 to -300 (nT)	Initial Phase duration (hrs)	Main Phase duration (hrs)	Recovery Phase duration (hrs)	Longevity of storm (hrs)	Type of storm	Asso. with Flares	Asso. with CIR	Types of CMEs
1	2	3	4	5	6	7	8	9	10	11	12
Solar Cycle 23					1996						
….	……	…….	………..	…Nil…	……	……	……	…..			
1997											
….	……	…….	………..	...Nil…	……	……	……	…..			
1998											
01	May 04	05UT	-205	14	04	84	102	938	X11	----Nil--	H
02	Sept. 24	09UT	-207	04	07	116	127	No CMEs	M71	-Nil--	--Nil---
1999											
03	Oct. 22	06UT	-237	05	04	102	111	No CMEs	M17	-Nil--	--Nil-
2000											
04	April 06	00UT	-288	04	09	132	145	1188	M10	-Nil--	H
05	Aug. 12	09UT	-235	06	06	99	111	1071	No Flare	-Nil--	-Nil--
06	Sept. 18	23UT	-201	03	02	89	95	1215	M33	-Nil--	H
2001											
07	April 11	23UT	-271	06	03	92	101	2411	X23	-Nil--	H
08	Nov. 06	06UT	-292	07	07	153	167	1810	X10	-Nil-	H
09	Nov. 24	16UT	-221	05	08	137	150	1443	M12		H
2002											
….	……	…….	………..	..Nil…	……	……	……	…..			
2003											
….	……	…….	………..	..Nil…	……	……	……	…..			
2004											
….	……	…….	………..	..Nil…	……	……	……	…..			
2005											
10	May 15	08UT	-263	01	03	114	118	1689	M14	---Nil---	H
11	Aug. 24	11UT	-216	01	04	77	82	2378	M26	---Nil---	H
2006											
….	……	…….	………..	..Nil…	……	……	……	…..			
2007											
….	……	…….	………..	..Nil…	……	……	……	…..			
Solar Cycle 24					2008						
….	……	…….	………..	..Nil…	……	……	……	…..			
2009											
….	……	…….	………..	..Nil…	……	……	……	…..			

2010											
….	……	…….	………..	..Nil…	……	……	……	…..			
2011											
….	……	…….	………..	..Nil…	……	……	……	…..			
2012											
….	……	…….	………..	..Nil…	……	……	……	…..			

Table 3. List of super great geomagnetic storms

Storm No.	Date of maximum decreases in Dst value	Time of Event	Magnitude of storm ≤-300 (nT)	Initial Phase duration (hrs)	Main Phase duration (hrs)	Recovery Phase duration (hrs)	Longevity of storm (hrs)	Type of storm	Asso. with Flares	Asso. with CIR	Types of CMEs
1	2	3	4	5	6	7	8	9	10	11	12
Solar Cycle 23						1996					
….	……	…….	………..	..Nil…	……	……	……	…..			
1997											
….	……	…….	………..	..Nil…	……	……	……	…..			
1998											
….	……	…….	………..	..Nil…	……	……	……	…..			
1999											
….	……	…….	………..	..Nil…	……	……	……	…..			
2000											
01	July 15	01UT	-301	05	07	73	85	1634	X19	--Nil-	H
2001											
02	March 31	08UT	-387	03	04	94	101	1072	X17	--Nil-	--Nil-
2002											
….	……	…….	………..	..Nil…	……	……	…….	…..			
2003											
03	Oct. 10	00UT	-353	10	02	17	29	2459	No Flare	--Nil-	H
04	Oct. 10	22UT	-383	04	04	82	90	No CMEs	X17	--Nil-	--Nil-
05	Nov. 20	20UT	-422	05	05	156	166	1824	M12	--Nil-	--Nil-
2004											
06	Nov. 08	06UT	-373	08	04	266	278	1215	X		
2005											
….	……	…….	………..	..Nil…	…….	……	……	…..			
2006											
….	……	…….	………..	..Nil…	……	……	……	…..			
2007											
….	……	…….	………..	..Nil…	……	……	……	…..			
Solar Cycle 24						2008					
….	……	…….	………..	..Nil…	……	……	……	…..			
2009											
….	……	…….	………..	..Nil…	……	……	……	…..			
2010											

….	……	…….	……..	..Nil…	……	……	……	…..			
2011											
….	……	…….	……..	..Nil…	……	……	……	…..			
2012											
….	……	…….	……..	..Nil…	……	……	…..	…..			

3. 11-Year solar activity variation

An indicator of the activity of the entire visible disc of the Sun is the relative sunspot number. The magnetic activity that surrounds sunspots can cause substantial variations in the ultraviolet and soft x-ray emission levels, despite the fact that sunspots themselves have extremely minimal effects on solar emissions. The upper atmosphere of the Earth is significantly impacted by these changes over the solar cycle [45-48]. Long-term variation was understood on the basis of the solar cycle variation of the solar output including solar wind using the interplanetary magnetic sector structure results from a variety of satellites and deep space probes [49-52]. The obvious cycle nature of sunspot number shows the average period of 11 years. Over the last six cycles this period has averaged 10.5 years. There is a good indication of a long-term cycle of approximately 70 years superimposed on the solar cycle [53, 54]. It is also evident that the rising phase (from minimum to maximum) is smaller than the declining (maximum to minimum) phase. Figure 1 displays the long-term monthly mean sunspot numbers. A surprising departure from solar maxima and minima is shown by the largest number of B-class flares that have been recorded three years following sunspot maxima that do not quite coincide with the phase of solar cycle 23 (figure 2). Total of 97 large geomagnetic storms (Dst-100nT) happened during the solar cycle's maximum and the lunar maximum (figure 3). A few geomagnetic storms are observed due to the presence of coronal holes and other solar activities near minimum phase. One year after sunspot maxima that don't quite coincide with solar cycle 23's phase, the strongest geomagnetic storms have been recorded. Solar cycle 23, which comes after the sunspot cycle, has only seen 5 C-class flares. From 1996 to 2012, 11 C-class flares and large geomagnetic storms (Dst-100nT) were detected (figure 4). The frequency of M-class flares peaked in 2002 (figure 5), two years following sunspot maxima, and it appears that this period does not correspond to the phase of solar cycle 23 for significant geomagnetic storms (Dst-100 to -200nT). M-class flare occurrence for superstorms (Dst-200nT) follows the phases of solar cycles 23 and 24. (figure 6). The frequency of X-class flares peaks in 2002, two years after the maximum of sunspot activity, and does not coincide with the part of solar cycle 23 that is characterized by moderate geomagnetic storms. Figures 7 and 8 depict the occurrence of X-class flares, which peak in 2001 (a year following sunspot maximums) and do not coincide with the phase of solar cycle 23 that is associated with powerful geomagnetic storms (Dst-100 to-200nT). The maximum occurrence of X-class flares for super storms (Dst-200 to -300nT) occurred in 2001, which did not follow the sunspot cycle, but geomagnetic storms were completely associated with X-class flares from 1996 to 2012 (figure 9). This flare maximum occurred in 2003, three sunspot maxima after the maximum, and did not follow the solar cycle 23 associated super great geomagnetic storms (Dst -300nT).

3.1. Association of M and X-class flare with CMEs for large geomagnetic storms (Dst≤-100 to -200nT)

Large geomagnetic disturbances are mostly caused by coronal mass ejections (CMEs) and corotating regions (CIRs), according to numerous recent research. Although prominence eruptions and solar flares are frequently linked, CMEs can sometimes happen without any of these events. The solar cycle affects the frequency of CMEs. In this part, we evaluate a series of 80 major geomagnetic storms that were reported during solar cycles 23 and 24 from 1996 to 2012 and were linked to Dst drops of less than -100nT to -200 nT. Numerous distinguishing characteristics, seasonal solar cycle dependence, fluctuation of various storm phases, and seasonal dependence of the aforementioned storm occurrences have all been examined.

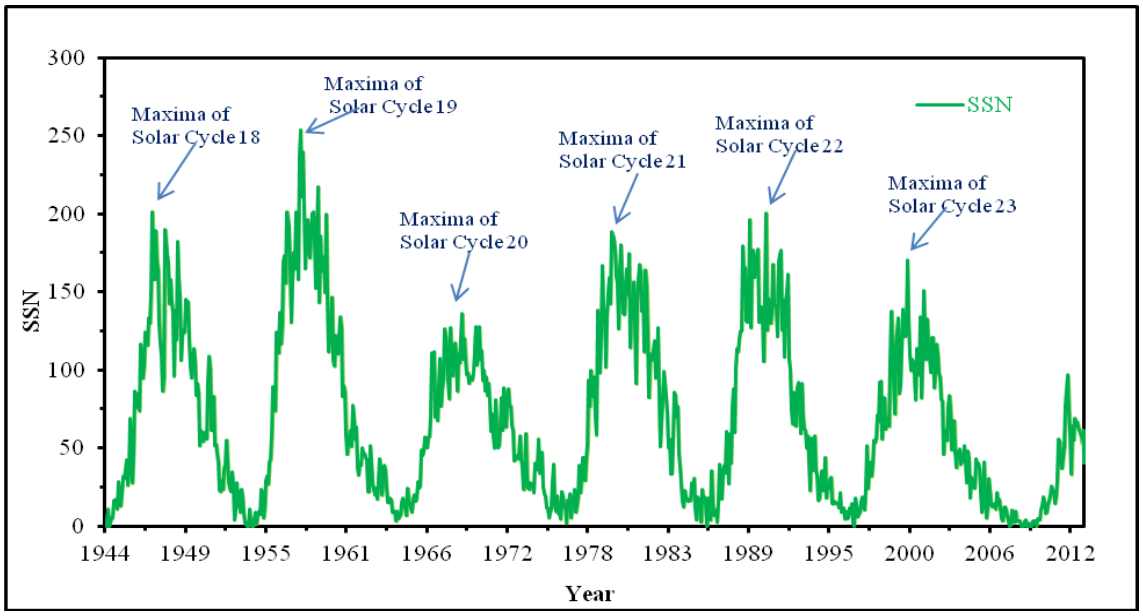

Figure 1. Graphs the Monthly Mean Sunspot Number from 1944 to 2012, which spans the 18–24 solar cycle.

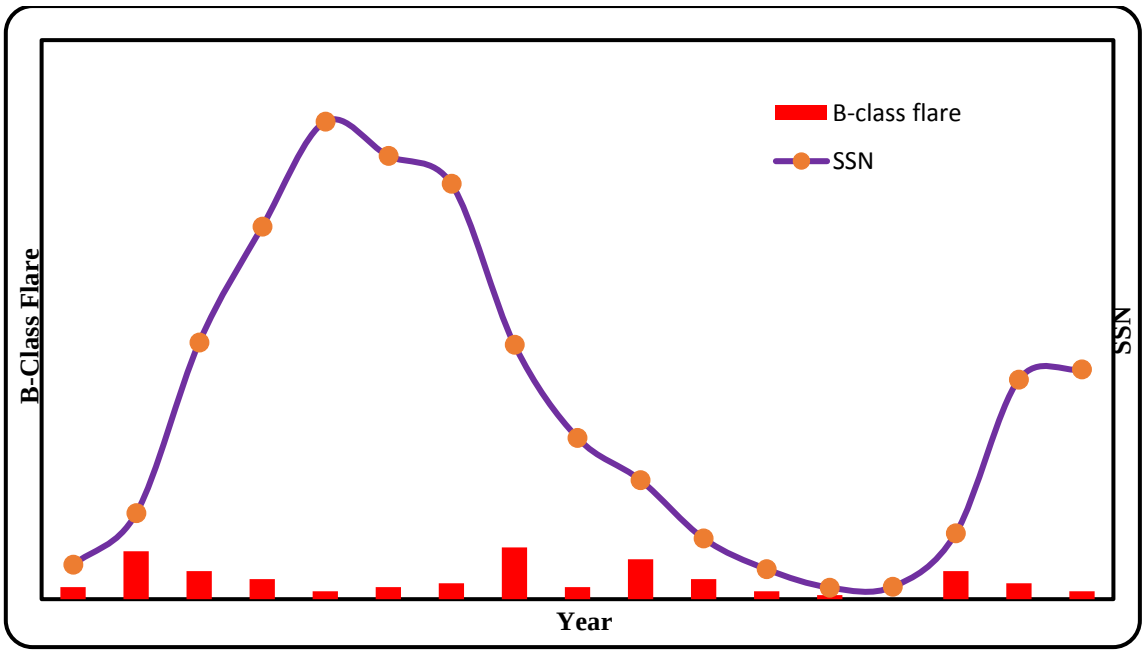

Figure 2. This graph displays the amount of sunspots and the frequency of B-class flares related with the mild GMSs from 1996 to 2012.

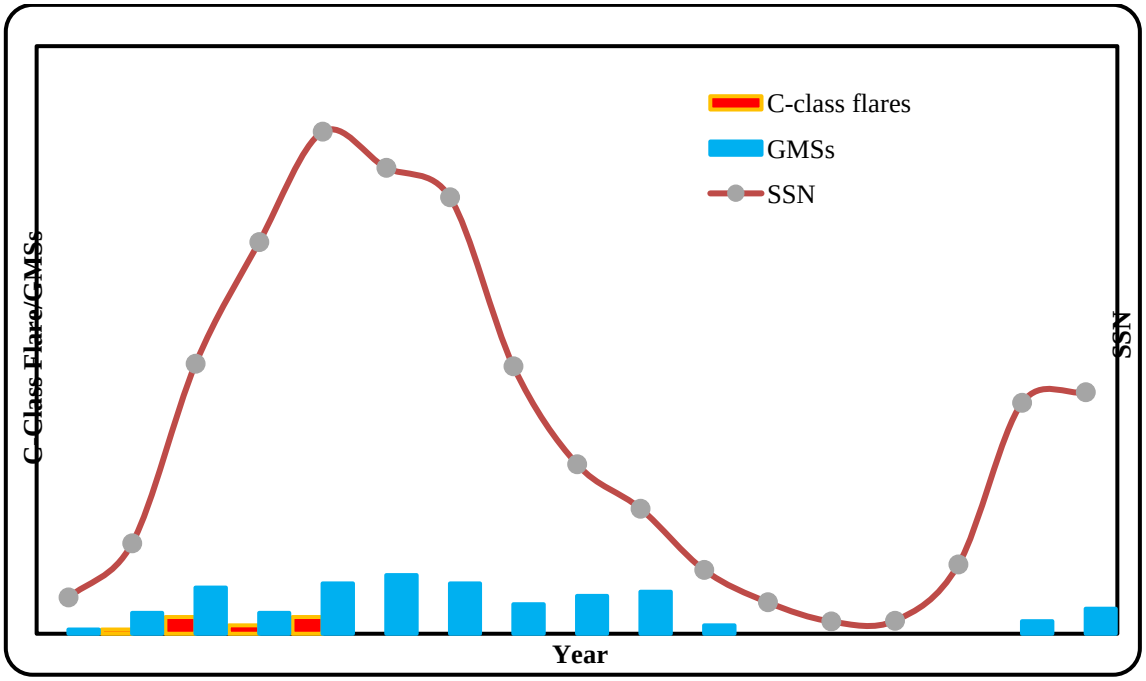

Figure 3. This graph displays the number of sunspots and the frequency of C-class flares connected to powerful geomagnetic storms (Dst -100 nT) from 1996 to 2012.

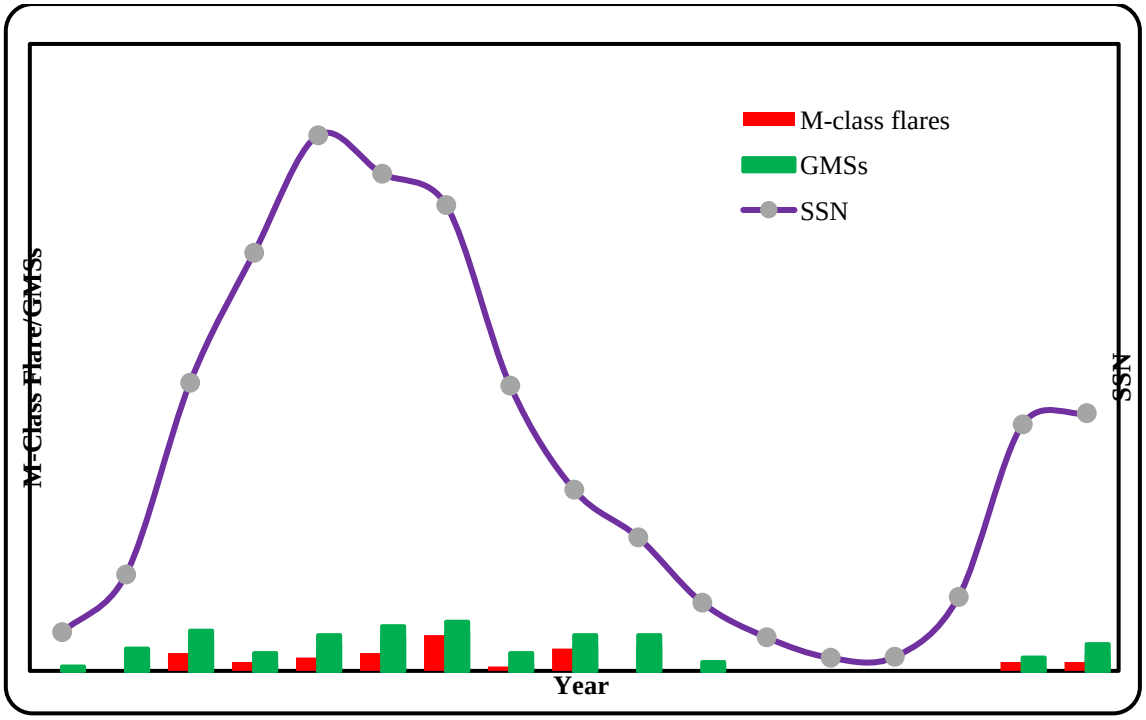

Figure 4. A graph showing the number of sunspots and the frequency of M-class flares associated with geomagnetic storms (Dst -100 to -200 nT) from 1996 to 2012 is shown.

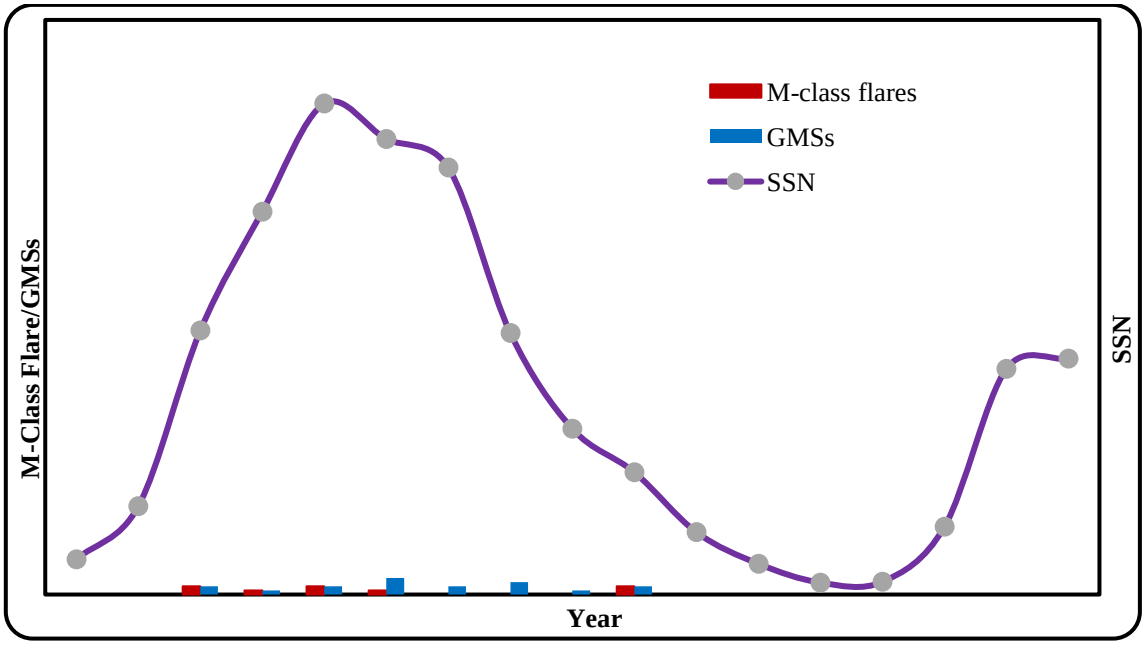

Figure 5. This graph depicts the number of sunspots and the occurrence of M-class flares connected to geomagnetic storms (Dst -200 nT) from 1996 to 2012.

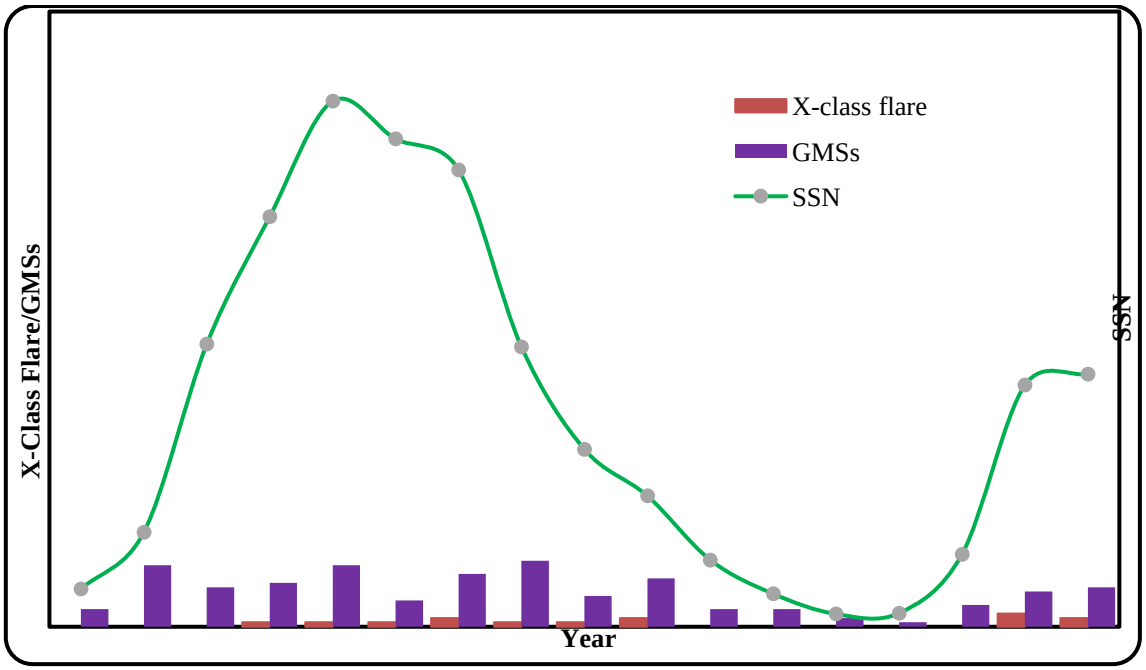

Figure 6. This graph depicts the sunspot number and occurrence of X-class flares connected to the moderate geomagnetic storms (Dst -60 to-100 nT) from 1996 to 2012.

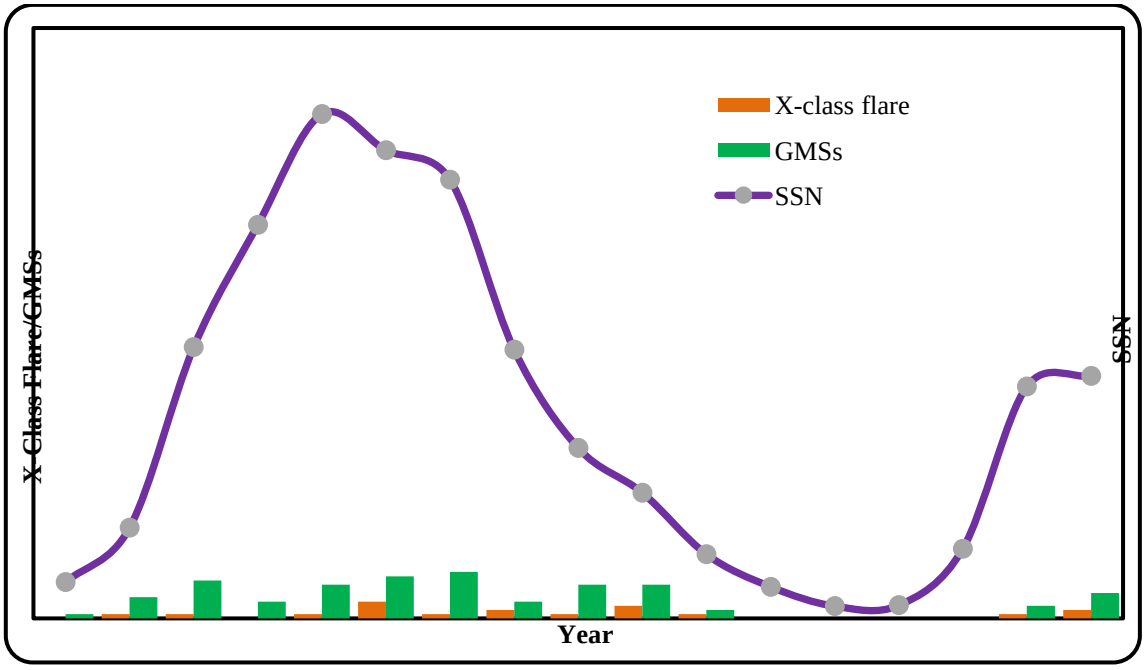

Figure 7. This graph depicts the number of sunspots and the frequency of X-class flares connected to powerful geomagnetic storms (Dst -100 to 200 nT) from 1996 to 2012.

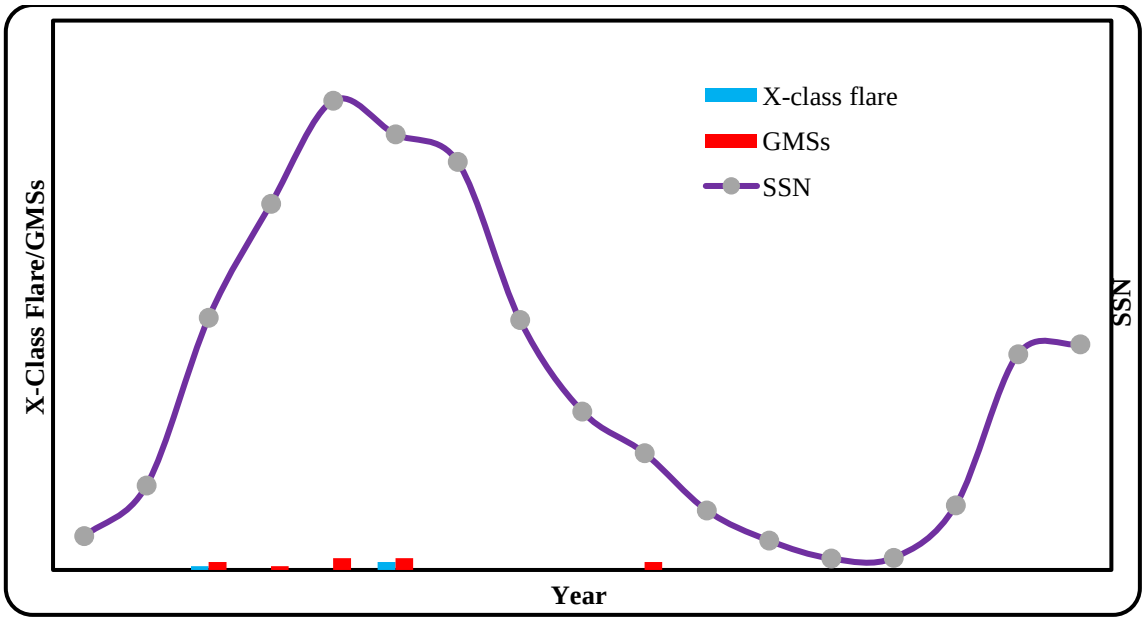

Figure 8. This graph shows the total number of sunspots and the frequency of X-class flares connected to super geomagnetic storms (Dst -200 to-300 nT) from 1996 to 2012.

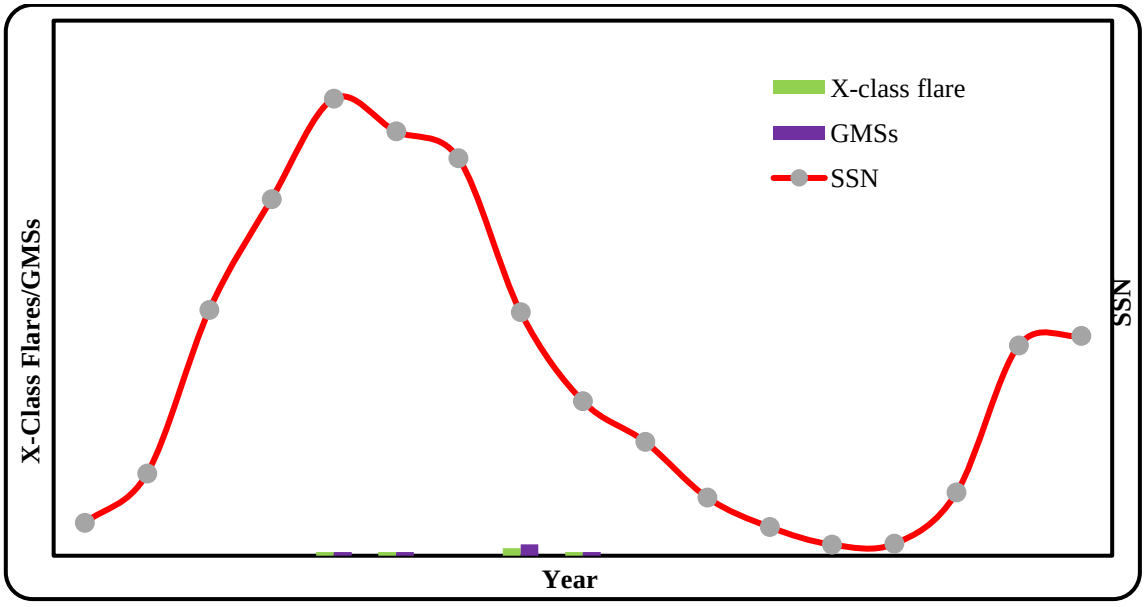

Figure 9. This graph depicts the number of sunspots and the frequency of X-class flares linked to the super-great geomagnetic storms (Dst -300 nT) from 1996 to 2012.

We observed that 52.5% (42/80) storms were associated with CMEs. Majority of these storms were associated with solar flares also. Number of storms related to M and X-class flares were 32.5% (26) and 20% (16) respectively, however 16.2% (13) storms were associated with CME only (without solar flares or CIR) and 13.7 (11) storms were associated with solar flares only (without association of CMEs or CIRs). It demonstrates that M-class and X-class flares frequently accompany major storms connected to CMEs (figure 10 and figure 11). Figure 12 depicts the maximum flare events in the years 1998 and 2002, which do not coincide with the solar cycle 23 phase. With one exception, CMEs do not follow the cycle's declination phase. We found that 17.5% (14/80) large storms were associated with CIR (Co-rotating interaction region). These storms were observed during solar minima of solar cycle 23 and 24 (figure 13).

3.2. Association of M and X-class flare with CMEs for super geomagnetic storms (Dst≤-200 to -300nT)

To access the level of association of flare with CMEs, we have considered super geomagnetic storms (Dst magnitude decreases less than -200 to -300nT) during the period 1996 to 2012 which cover the solar cycle 23 and maxima of 24. The solar plasma is heated and accelerated during solar flares and coronal mass ejections, resulting in intense outbursts known as solar energetic particle (SEP) events (CMEs). Forbush [55] noted the first observation of SEP events as a rapid increase in the intensity of the ground-level ion chamber during massive solar flares that occurred in February and March 1942.

Total 11 super geomagnetic storms were observed during the period 1996-2012. It was discovered that 8 out of 11 storms had a 72.7% CME association. The majority of these storms also had solar flares as a contributing factor. However, 9% (1) of storms had CMEs only (without solar flares or CIR) and 18.1% (2) of storms had flares exclusively. The percentage of storms associated with M and X-class flares was 45.4% (5) and 27.2% (3), respectively (without association of CMEs). It demonstrates that superstorms connected to CMEs are more frequently accompanied by M- and X-class flares, which showed in (figure 14). This figure reveals that t M-class flares has two peaks one was in solar maxima and second in declining phase of solar cycle 23. However, X-class flares follow the sunspot cycles.

3.3. Association of M and X-class flare with CMEs for super great geomagnetic storms (Dst≤-300nT)

Geomagnetic storms are periods of time during which a sufficiently strong and long-lasting interplanetary convective electric field causes an intensified ring current to exceed a critical storm time Dst index threshold through a significant energy injection into the magnetosphere-ionosphere system. Technology and systems like satellites, GPS, and radio communications are affected by solar flares, coronal mass ejections (CMEs), and the solar wind. Therefore, the military, aviation, energy transfer, and the communications industries all depend heavily on space weather forecasts.

In this section we have studied super great geomagnetic storms (Dst≤-300nT) and association of M, X-class flare with CMEs during the period 1996 to 2012. We have observed six super great geomagnetic storms during this period. We have identified their solar and interplanetary causes. These storms were related to CMEs observed by the Large Angle and Spectroscopic Coronagraph (LASCO). Out of six storms, 1 associated with CMEs only and 4 associated with CMEs + flare and one storm associated with flare only. We have observed only one M-class flare and the association of CMEs with M-class flare does not follow the phase of solar cycle 23 because it is maximum in year 2003, three after maxima of sunspot cycle.

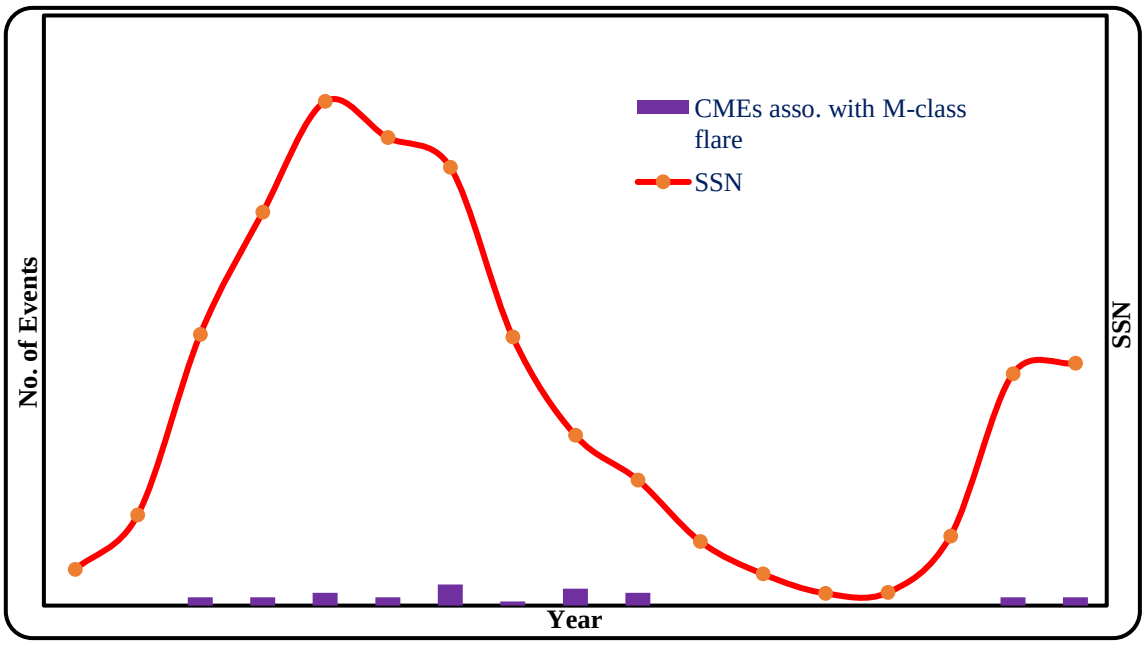

Figure 10. This graph shows the occurrence of M-class flare associated with CMEs and SSN for large storms (Dst ≤-100 to -200 nT) during the period 1996 to 2012.

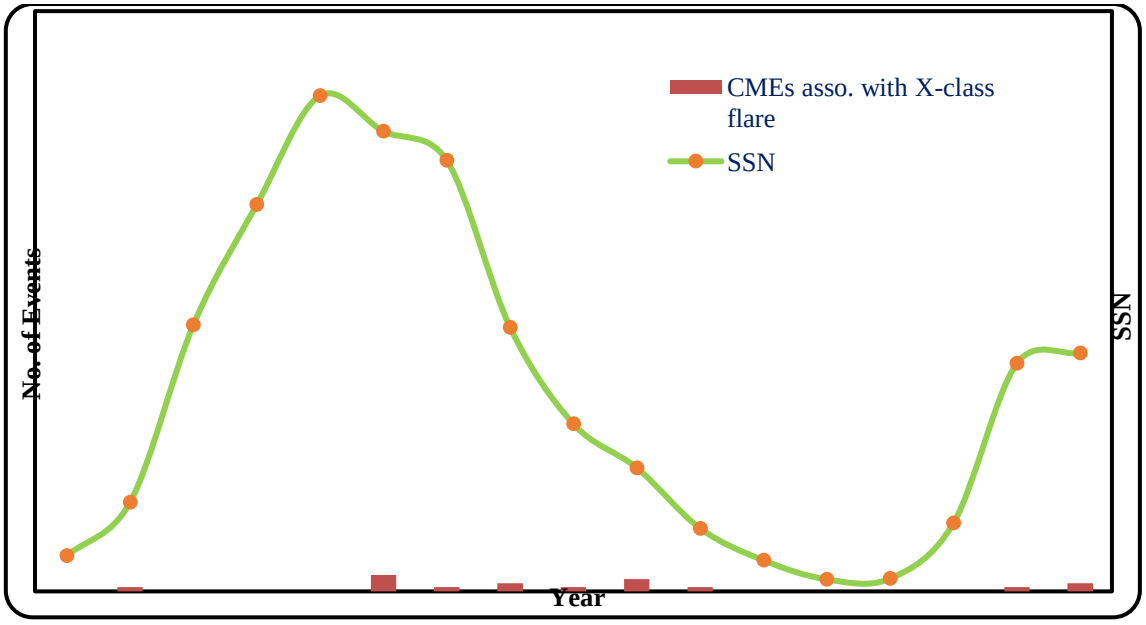

Figure 11. This graph displays the frequency of X-class flares related with CMEs and SSN for major storms (Dst -100 to -200 nT) from 1996 to 2012.

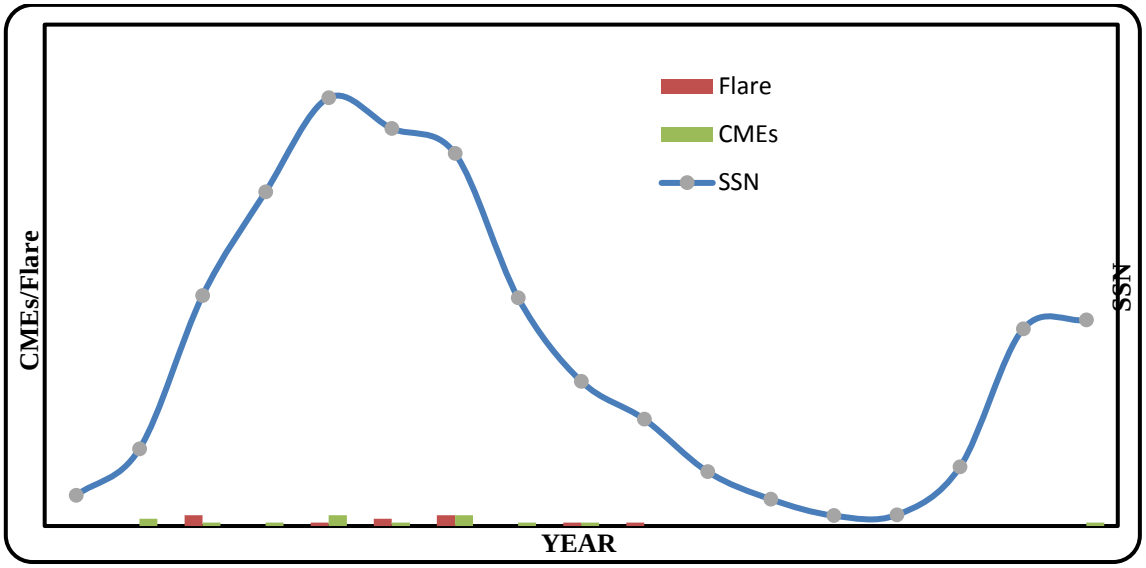

Figure 12. This graph shows the occurrence of CMEs, Flare and SSN for large storms (Dst ≤ -100 to -200nT) during the period 1996 to 2012.

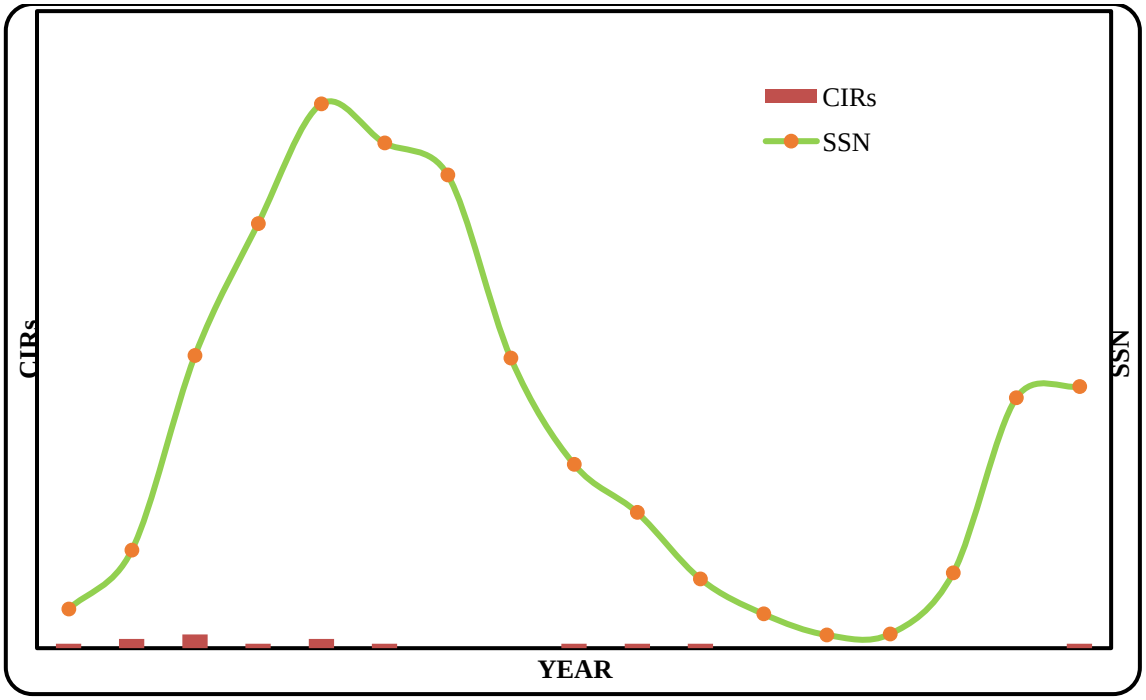

Figure 13. This graph shows the occurrence of CIRs and SSN for large storms (Dst ≤-100 to -200nT) during the period 1996 to 2012.

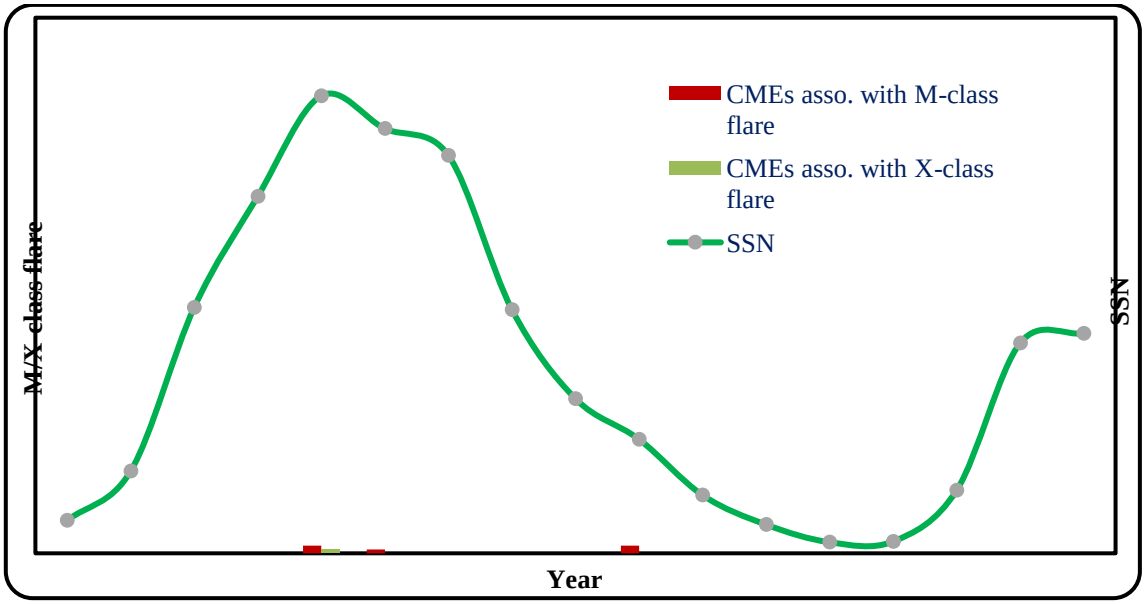

Figure 14. This graph shows the occurrence of M and X-class flare associated with CMEs and SSN for super storms (Dst ≤-200 to -300 nT) during the period 1996 to 2012.

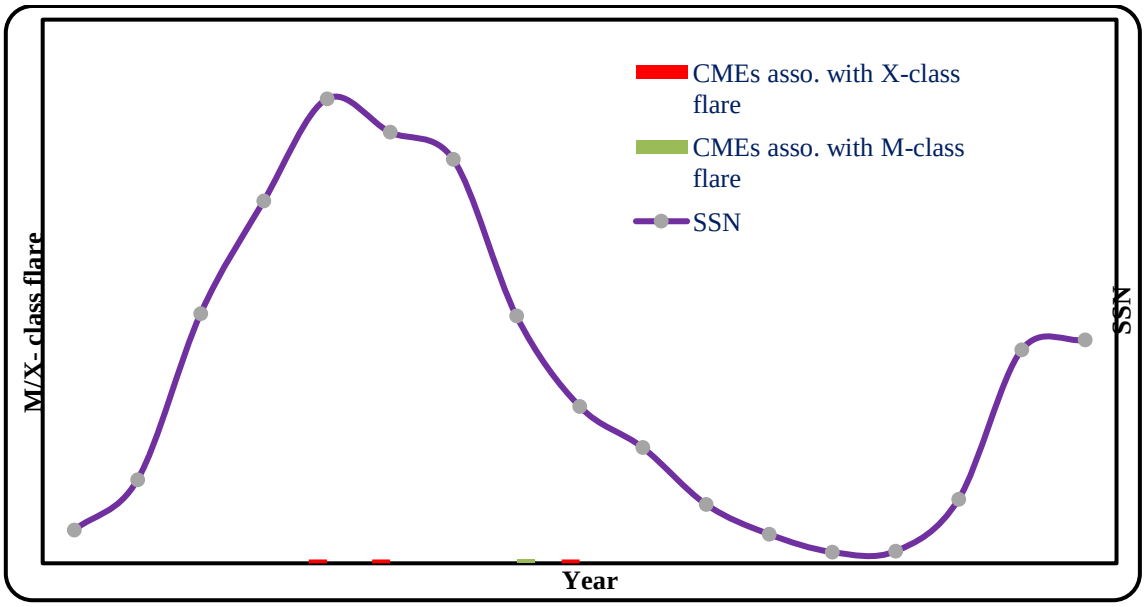

Figure 15. This graph shows the occurrence of M and X-class flare associated with CMEs and SSN for super storms (Dst ≤-300 nT) during the period 1996 to 2012.

The association of X-class flares with CMEs maximum in year 2003 which is three after maxima of sunspot cycle (Figure 15) We found that 4 out of 6 storms (66.6%) had CMEs as a contributing factor. The majority of these storms also had solar flares as a contributing factor. There were 16.6% (1) storms connected to M-class flares and 50% (3) connected to X-class flares, respectively. However, 16.6% (1) storms were connected to CMEs alone (without solar flares or CIR) and 16% (1) storms were connected to flares alone (without association of CMEs). It demonstrates that super-strong storms connected to CMEs are more frequently followed by M- and X-class flares.

4. Conclusion

Geomagnetic storms, which are observable on Earth's surface as disturbances in the geomagnetic field's constituent sections, are caused by electric currents moving in the magnetosphere and upper atmosphere. Understanding the solar and planetary processes that lead to the geomagnetic activity is a difficult task for solar-terrestrial physicists. The geomagnetic field is disturbed by the solar output, more precisely by the discharge of solar plasma and magnetic field into the interplanetary medium. Also, intriguing is the transfer of plasma and energy from the Sun to Earth. Geomagnetic storms can occur in a variety of ways, and many studies have examined their various solar and planetary sources. Considering the latest theories and mechanisms, we have analyzed moderate, large, super and super great geomagnetic storms associated with Dst decrease of more

than 100nT, 200nT, 300nT respectively and its various associations. For this study, we have chosen a large interval from 1996 to 2012 covering solar cycle 23 and current cycle 24.

On the basis of the results and discussion as described in the paper, we have provided the following summary of key findings from the examination of geomagnetic storms (of magnitude -100 nT, -200 nT, and -300 nT) and their correlation with interplanetary parameters for the years 1996 to 2012

We discovered that CIR was connected to 17.5% (14/80) of significant geomagnetic storms (Dst-100 to -200nT) (Co-rotating interaction region). Large storms were discovered to be mostly caused by solar flares (M- and X-class), while a significant portion of these storms were also caused by CIR. In solar cycle 23–24, these storms were seen during solar minima. We have observed that 72.7% (8/11) super geomagnetic storms (Dst≤-200 to -300nT) were connected to flares and CMEs. M-class and X-class flares are more frequently present in superstorms connected to CMEs.

It is observed that 66.6% (4/6) super great geomagnetic storms (Dst≤-300nT) were associated with CMEs and solar flares. Number of storms related to X-class flares or CMEs were 50% (3/6). X-class flare/CMEs are found to be responsible for super geomagnetic storms.

In the majority of geomagnetic storms the initial phase lies between 0-3 hours, and the main phase duration for the maximum number of major storms lies between 0-8 hours, whereas recovery phase duration lies between 0-2 days for majority of the events.

It has also been discovered that the main phase's duration is no greater than the recovery phase's.

As an indicator of the magnetospheric compression caused by an increase in solar wind velocity, Dst declines with rising magnetopause shielding currents.

A new useful metric to measure solar geoeffectiveness is provided by the physical connection between CMEs and geomagnetism. These outcomes match those that were anticipated in the previous research [26-27, 32, 39]. As discussed by Richardson [32] Geomagnetic activity associated with streams is typically associated with intermittent intervals of southward fields associated with large amplitude Alfvenic fluctuations [27, 29]. When it comes to modelling research and space weather phenomena, these quantitative relationships are essential.

Conflict-of-interest statement

The authors have no conflicts of interest to declare.

Authors have seen and agree with the contents of the manuscript and there is no financial interest to report. We certify that the submission is original work and is not under review at any other publication.

References

1. N U Crooker, *J. Atmo. Sol-Terr. Phys.* **62** (2000)1071.
2. S C Dubey and A P Mishra, *Earth Moon Planets* **84** (2000) 34.
3. E Echer, V M Alves and W D Gonzalez, *J. Atmo. Sol-Terr. Phys.* **67** (2005) 839.
4. E Echer, et al., *JGR.* **113**, 1 (2008b) A05221.
5. E Echer, B T Tsurutani, and W D Gonzalez, *Sol. Terr. Phys*. **73** (2011)1454.
6. T N Davis and M Sugiura, *JGR.* **71** (1996) 785.
7. T G Forbes, *JGR.* **89** (2000) 21.
8. W D Gonzalez and B T Tsurutani, *Planet. Space Sci.* **35** (1987).
9. J T Gosling, et al., *GeoRL*. **17** (1990) 901.
10. J T Gosling, et al., *JGR*. **96** (1991) 7831.
11. W D Gonzalez, et al., *GeoRL.* **34** (2007).
12. A J Hundhausen, *J. Geophys. Res*. **98** (1993) 13177
13. R P Kane, *JGR.* **82** (1977) 561.
14. T Iyemori and D R K Rao, *AnGp.* **14** (1996) 608.
15. V I Makarov and K R Sivaraman, *Solar Phys.* **123** (1989b) 367.
16. R F Muscheler, et al., *Quat. Sci. Rev*. **26** (2007) 82.
17. V N Obridko, et al., *Solar Phys.* **281** (2012) 779.
18. V N Obridko and B D Shelting, *Solar Phys*. **270** (2011) 297.
19. V N Obridko, *et al.*, *Sol Phys* **281** (2012) 779
20. I G Richardson and H V J. Cane, *J. Space Weather Space Clim.* **2** (2012) A02.
21. I G Richardson, *J. Space Weather Space Clim.* **3** (2013) A08.
22. S Singh, D Shrivastava and A P Mishra, *Indian J. Sci. Res.* **3** (2012) 121.
23. S Singh, et al., *IJPA.* **1** (2012) 1103.
24. N Srivastava, *AnGeo.* **23** (2005) 2989.
25. S Singh and A P Mishra, *Indian J. Phys.* **93**, 2 (2019) 139.
26. S Singh and A P Mishra, *Indian J. Phys.* **89** (2015) 1227.
27. B T Tsurutani, et al., *JGR* **93** (1988) 8519.
28. N Gopalswamy, et al., *Ann. Geophys.* **26**, 10 (2008) 3033.
29. S W Kahler, *J. Geophys. Res.* **106**, A10 (2001) 20947.
30. H V Cane, I G Richardson, and T T von Rosenvinge, *J. Geophys. Res.* **115** (2010) A08101.
31. J Hwang, et al., *Acta Astronaut.* **67**, 3 (210) 353.
32. I G Richardson, *J. Space Weather Space Clim.* **3** (2013) A08.

33. Z Mohammadi, et al., *J. Geophys. Res.* **126**, 7 (2021) e2020JA028868.
34. B T Tsurutani, et al., *GeoRL.* **19** (1992) 73.
35. I G Usoskin, et al., *Astrophys. J.* **700**, 2 (2009) L154.
36. W D Gonzalez, et al., *SSRv.* **158** (2011) 69.
37. A Belov, et al., *Cosmic Res.* **43**, 3 (2005) 165.
38. D F Webb and R A Howard, *JGR.* **99** (1994) 4201.
39. D F Webb, *Rv Geo.* **33** (1995) 577.
40. Y Zhang, et al., *Solar Phys.* **241** (2007) 329.
41. X Luo, et al., *MDPI.* **18**, 6 (2018) 1784.
42. J Feynman and S B Gabriel, *J. Geophys. Res.* **105**, A5 (2000) 10543.
43. D M Oliveira, et al., *Space Weather* **16 (**2018) 6.
44. J M Wilcox and D S Colburn, *Rv Geo.* **75** (1970) 6366.
45. S Taran, et al., *Adv. Space Res.* **71**, 12 (2023) 5453.
46. J C Zhang, et al., *JGR.* **111** (2006) 1.
47. A R Choudhari, *Cur. Ent. Sci.* **74** (1998) 478.
48. S Watari, *Earth Planets Space* **69** (2017) 70.
49. P F Chen, *Living Rev. Solar Phys.* **8** (2011) 1.
50. S Yashiro, et al., *J. Geophys. Res.* **110** (2005) A12S05.
51. R L Moore, et al., *J. Astrophys.* **552** (2001) 833.
52. J Lin, *Chin. J. Astron. Astrophys.* **2** (2002) 539.
53. J Lin and T G Forbes. *J. Geophys. Res.***105** (2000) 2375.
54. J Wang, et al., *Sol. Phys.* 244 (2007) 75.
55. S E Forbush, *Phys. Rev.* **70** (1946) 771.